

Supporting Information for the Article:

Phase Selection during the Crystallization of Metal-Organic Frameworks; Thermodynamic and Kinetic Factors in the Lithium Tartrate System

5

Hamish Hei-Man Yeung and Anthony Kevin Cheetham*

Department of Materials Science and Metallurgy, University of Cambridge, Pembroke Street, Cambridge, U.K., CB2 3QZ.

Contents.

10 S1. Materials and methods.

Table S1. Table of yields and morphologies from lithium tartrates phase behavior experiments.

Figure S1. Powder X-ray diffraction of the source reaction of dilithium d,L-tartrate dihydrate, **10**, containing approximately 50 % **8**, 40 % **10** and 10 % **5**.

15 Figure S2. Powder X-ray diffraction of the source reaction of dilithium *meso*-tartrate dihydrate, **11**, after standing in ambient conditions, containing pure **7**.

Figure S3. Powder X-ray diffraction of the products from phase investigation reactions of lithium tartrates, from *meso*-tartaric acid in ethanol, showing phases in order of abundance.

Figure S4. Powder X-ray diffraction of the products from phase investigation reactions of lithium tartrates, from *meso*-tartaric acid in water:ethanol, 20 showing phases in order of abundance.

Figure S5. Powder X-ray diffraction of the products from phase investigation reactions of lithium tartrates, from L-tartaric acid in ethanol, showing phases in order of abundance.

Figure S6. Powder X-ray diffraction of the products from phase investigation reactions of lithium tartrates, from L-tartaric acid in water:ethanol, showing phases in order of abundance.

25 Figure S7. Powder X-ray diffraction of the products from phase investigation reactions of lithium tartrates, from d,L-tartaric acid in ethanol, showing phases in order of abundance.

Figure S8. Powder X-ray diffraction of the products from phase investigation reactions of lithium tartrates, from d,L-tartaric acid in water:ethanol, showing phases in order of abundance.

S1. Materials and methods

30 Synthesis.

All reagents, lithium acetate dihydrate (98 %, Fisher Scientific UK), D,L-tartaric acid (99.5 %, Fisher Scientific UK), L-tartaric acid (>99 %, Fisher Scientific UK) and *meso*-tartaric acid monohydrate (\geq 97 %, Sigma-Aldrich), and solvents, ethanol (reagent grade, Fisher Scientific UK) and in-house deionized water were used as received under aerobic conditions. Reactions were carried out in 12 mL borosilicate glass vials with PTFE-lined caps (Fisher Scientific UK) and 23 mL PTFE-lined stainless steel autoclaves obtained from Parr

35 Instrument Company.¹⁹

Phase behavior from ethanol.

In the case of L- and *meso*-tartrates, their respective acids (1 mmol) were placed in a 12 mL vial with lithium acetate dihydrate (2 mmol) and ethanol (10 mL), and the mixture left to stand at room temperature. Similar reactions were prepared and placed in ovens at various temperatures up to 200 °C, using autoclaves as vessels above 60 °C. After three days the reactions were cooled to 25 °C and the contents 40 were filtered, washed in ethanol and dried in air. Products were colorless crystals and/or white powders with yields of 88 mg – 157 mg (54 % - 97 % for Li₂C₄H₄O₆). Due to the low solubility of d,L-tartaric acid in ethanol, reactions involving d,L-tartrates were made up by layering a solution of L-tartaric acid (0.5 mmol) and d-tartaric acid (0.5 mmol) in ethanol (5 mL) on top of a solution of lithium acetate dihydrate (2 mmol) in ethanol (5 mmol). Products were colorless crystals and/or white solids with yields of 30 mg - 116 mg (19 % - 72 % for Li₂C₄H₄O₆).

45 Phase behavior from water:ethanol.

In the case of L- and d,L-tartrates, a solution of lithium acetate dihydrate (2 mmol) in water:ethanol (1:2, 5 mL) was layered under a solution of the respective acid (1 mmol) in water:ethanol (1:4, 5 mL) in a 12 mL vial and the reaction was left to stand at 25 °C. Similar reactions were prepared and placed in ovens at various temperatures up to 200 °C, using autoclaves as vessels above 60 °C. After 3-4 days the reactions were cooled to 25 °C and the contents were filtered, washed in water:ethanol (1:4) and dried in air. Products were 50 colorless crystals and/or white solids with yields of 27 mg - 98 mg (17 % - 60 % for Li₂C₄H₄O₆). Due to the more rapid precipitation of *meso*-tartrates, in this case the reaction mixtures were prepared using a solution of *meso*-tartaric acid (1 mmol) in water:ethanol (1:2, 5 mL). Products were colorless crystals and/or white solids with yields of 91 mg - 125 mg (56 % - 77 % for Li₂C₄H₄O₆).

Single crystals of [Li₂(d,L-C₄H₄O₆)(H₂O)₂] in P1, **10**.

A solution of lithium acetate dihydrate (2 mmol) in water:ethanol (1:2, 5 ml) was layered under a solution of d,L-tartaric acid (1 mmol) in

water:ethanol (1:4, 5 ml) in a 4 ml borosilicate vial, which was left to stand at 20 °C. After 6 days the precipitate, a mixture of colorless triangular prisms and needles, was separated from the mother liquor. A suitable triangular prism was selected for structure determination of Li₂(d,l-C₄H₄O₆)(H₂O)₂, **10**. Powder X-ray diffraction analysis (see SI) showed a mixture of **8** and **10**, with trace amounts of **5**, but a phase-pure sample could not be obtained.

5 Single crystals of [Li₂(meso-C₄H₄O₆)(H₂O)_{0.5}] in C222₁, **11**.

A solution of lithium acetate dihydrate (2 mmol) in water:ethanol (1:2, 5 ml) was layered under a solution of meso-tartaric acid (1 mmol) in water:ethanol (1:4, 5 ml) in a 4 ml borosilicate vial, which was left to stand at 20 °C. After 6 days the precipitate, consisting of colorless square plates surrounded by polycrystalline material, was separated from the mother liquor and a suitable square plate was selected for structure determination of Li₂(meso-C₄H₄O₆)(H₂O)_{0.5}, **11**. The remaining precipitate was left to stand in air over two months, yielding a white powder, which was found to consist of pure Li₂(meso-tart), **7**, by powder X-ray diffraction (see SI). A pure sample of **11** could not be obtained. Elemental analysis found C 29.43 %, H 2.51 % (calculated C 29.67 %, H 2.49 %).

Crystal Structure Determinations.

The relevant details of structure determinations are presented in the Supporting Information. Crystal structure determination by X-ray diffraction was performed on an Oxford Diffraction Gemini E Ultra diffractometer equipped with dual source Cu radiation ($\lambda = 1.54184$ Å, operating at 40 kV and 40 mA with confocal mirrors to increase flux) and Mo radiation ($\lambda = 0.7107$ Å, operating at 50 kV and 40 mA). Data were collected at 120 K using ω scans and the mean detector area resolution was 10.4 pixels mm⁻¹. Data collection, cell determination and refinement, intensity integration and face indexation were performed using CrysAlisPro software.²⁰ Structures were solved by direct methods and full matrix least-squares refinements against | F^2 | were carried out using the SHELXTL-PLUS package of programs²¹ within the WinGX interface.²² All non-hydrogen atoms were refined anisotropically; hydrogen atoms were then inserted using a riding model and refined with isotropic displacement parameters constrained to 1.2 and 1.5 times those of their adjacent carbon (non-methyl), and oxygen and methyl carbon atoms, respectively. Visualization of structures was carried out using Diamond²³ and Mercury²⁴ programs.

Powder X-ray Diffraction.

Data were collected on a Bruker D8 theta/theta (fixed sample) diffractometer with LynxEye position sensitive detector, in Bragg Brentano parafocusing geometry, reflection mode using Cu K α radiation ($\lambda = 1.5418$ Å). Scans were taken over an angular range of 5° - 60° (2θ) with step size 0.01°. Analysis of the data was carried out using the X'Pert HighScore Plus program.²⁵

References

- 19 Parr Instrument Company, 211 53rd St., Moline, Illinois 61265 USA.
- 20 CrysAlis CCD, CrysAlis RED and associated programs, Oxford Diffraction Ltd., Abingdon, U.K., 2006.
- 21 G. M. Sheldrick, *Acta Crystallogr., Sect. A: Found. Crystallogr.* 2008, **64**, 112-122.
- 22 L. J. Farrugia, *J. Appl. Crystallogr.*, 1999, **32**, 837-838.
- 23 K. Brandenburg and H. Putz, *Diamond*, 3.2; CRYSTAL IMPACT GbR, Bonn, Germany, 2009.
- 24 C. F. Macrae, P. R. Edgington, P. McCabe, E. Pidcock, G. P. Shields, R. Taylor, M. Towler and J. van de Streek, *J. Appl. Crystallogr.*, 2006, **39**, 453-457.
- 25 X'Pert HighScore Plus, 2.0; PANalytical B.V., Almelo, The Netherlands, 2004.

Table S1. Table of yields and morphologies from lithium tartrates phase behavior experiments. Phases are listed in order of abundance, with major, minor and trace phases in bold, italics and parentheses, respectively.

Ligand isomer	Solvent	Synthesis temperature (°C)						
		25	60	100	125	150	180	200
L-	ethanol	3, (2) powder [94 %]	3, 2 powder [94 %]	2, 3 needles [86 %]	2, 3 needles [85 %]	2, 3 plates, powder [82 %]	2, (3) needles [82 %]	2 needles [88 %]
L-	water / ethanol	2, 13 plates	2, (9) plates [60 %]	2, 9 plates	2, 9 plates, rods [54 %]	2, (9) plates, rods [52 %]	2, 6, (9) polycr. [59 %]	2, 6, (9) polycr. [56 %]
meso-	ethanol	?	7, 6, (?) powder, blocks [77 %]	7, 6 powder, rods [57 %]	7, 6 powder, rods [54 %]	7, 4, 6 powder, rods [77 %]	7, 4, 6 powder, needles [85 %]	6, 7, 4 needles, powder [80 %]
meso-	water / ethanol	7, 6 polycr. [?? %]	7, 6 plates [59 %]	6 blocks [56 %]	6 rods [77 %]	6 rods [77 %]	6 rods [73 %]	6 rods, polycr. [68 %]
D,L-	ethanol	13, ? powder	5, 8, (?) rods, powder [62 %]	5, 8 needles [62 %]	n/a	5, 8 needles [19 %]	5 powder, needles [69 %]	5 powder, needles [72 %]
D,L-	water / ethanol	13 plates	8, 5 rods, plates [17 %]	8 rods [19 %]	8 rods [20 %]	8 rods [20 %]	8, 6 rods, polycr. [22 %]	6 polycr. [31 %]

Figure S1. Powder X-ray diffraction of the source reaction of dilithium d,l-tartrate dihydrate, **10**, containing approximately 50 % **8**, 40 % **10** and 10 % **5**.

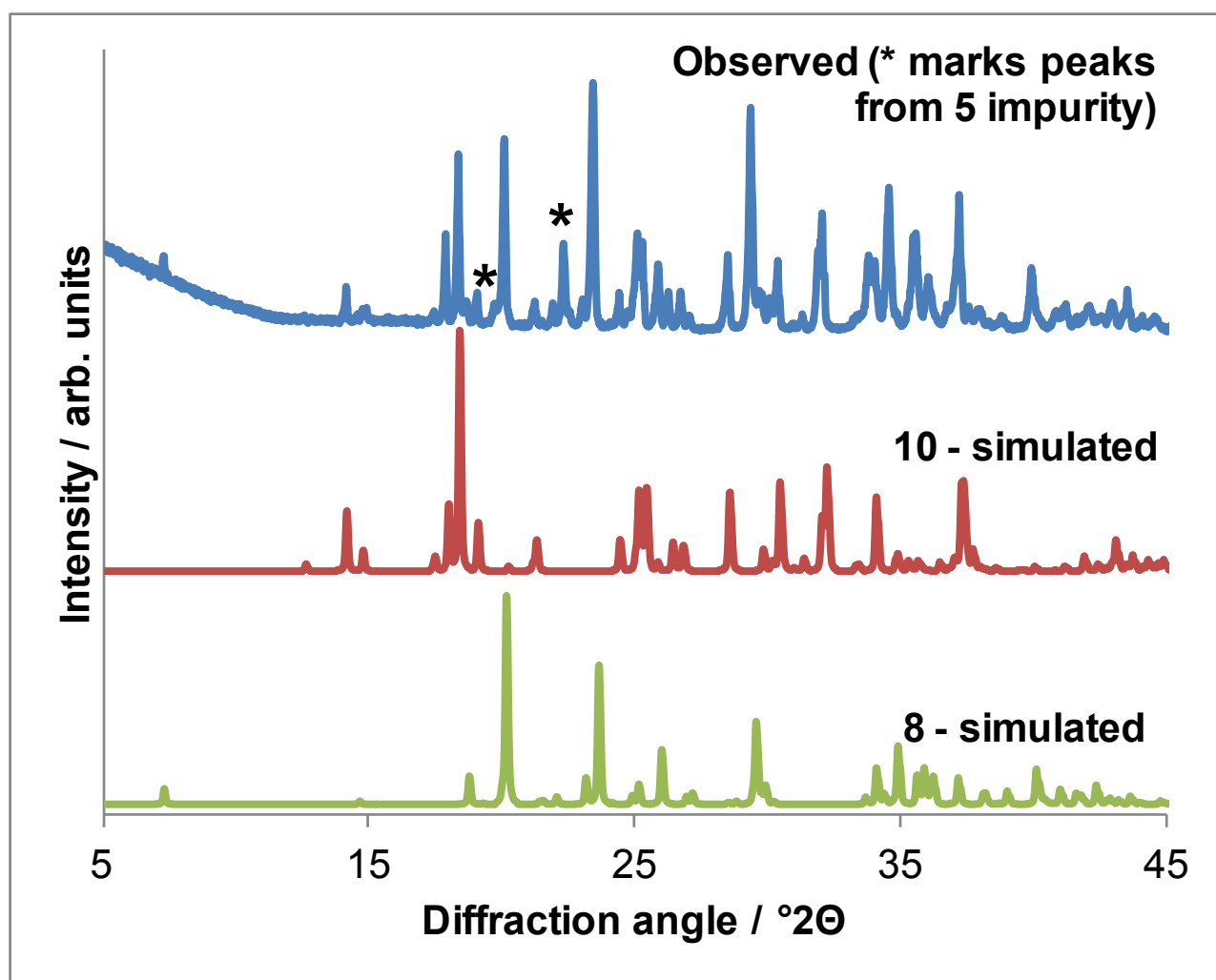


Figure S2. Powder X-ray diffraction of the source reaction of dilithium *meso*-tartrate dihydrate, **11**, after standing in ambient conditions, containing pure **7**.

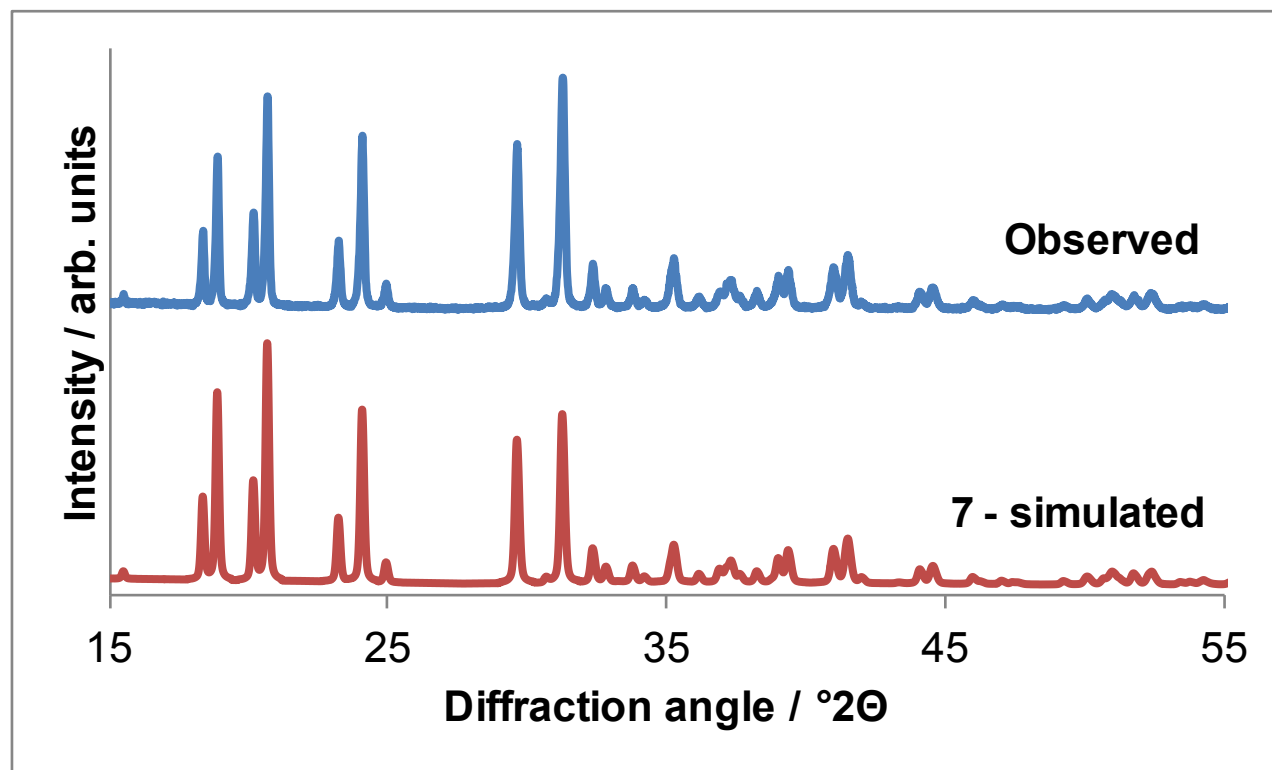


Figure S3. Powder X-ray diffraction of the products from phase investigation reactions of lithium tartrates, from *meso*-tartaric acid in ethanol, showing phases in order of abundance.

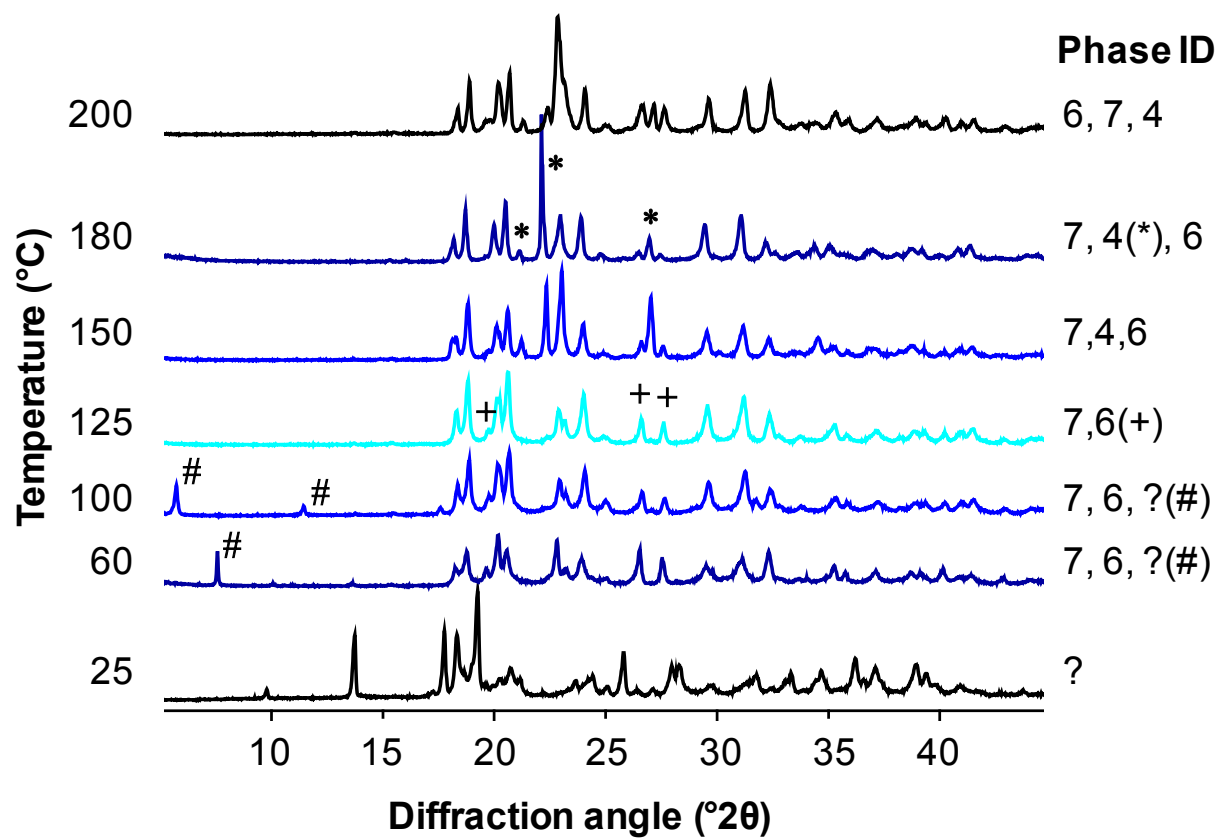


Figure S4. Powder X-ray diffraction of the products from phase investigation reactions of lithium tartrates, from *meso*-tartaric acid in water:ethanol, showing phases in order of abundance.

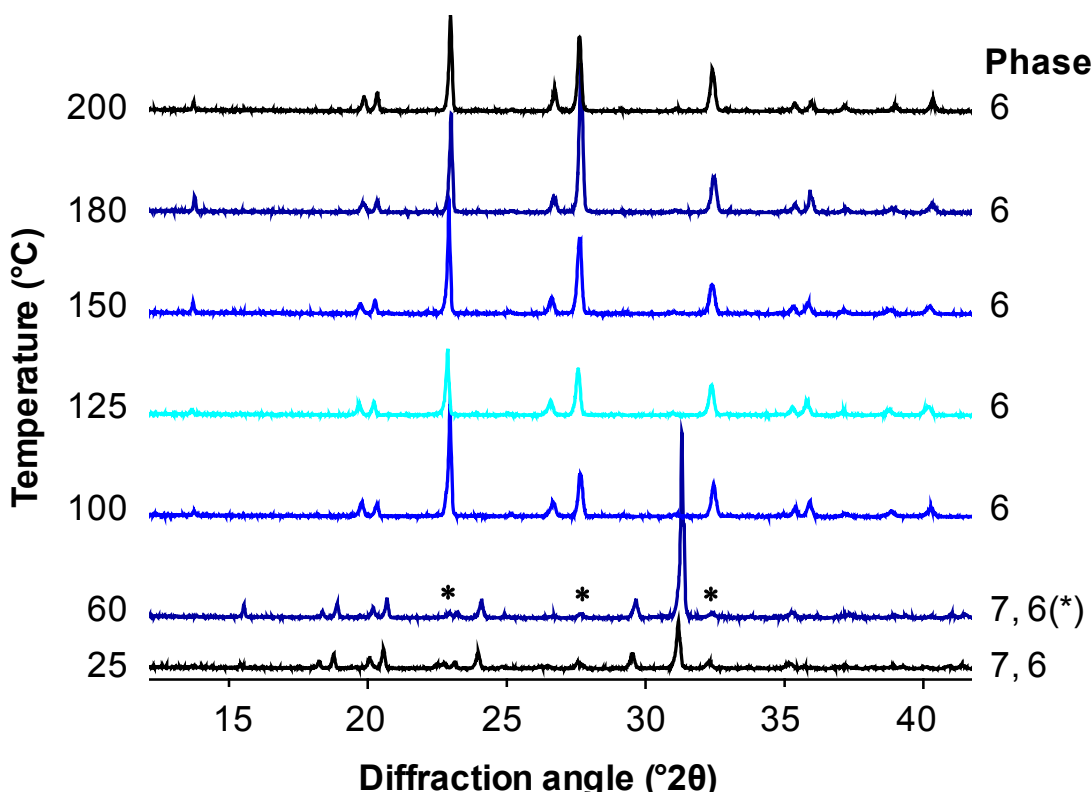


Figure S5. Powder X-ray diffraction of the products from phase investigation reactions of lithium tartrates, from L-tartaric acid in ethanol, showing phases in order of abundance.
5

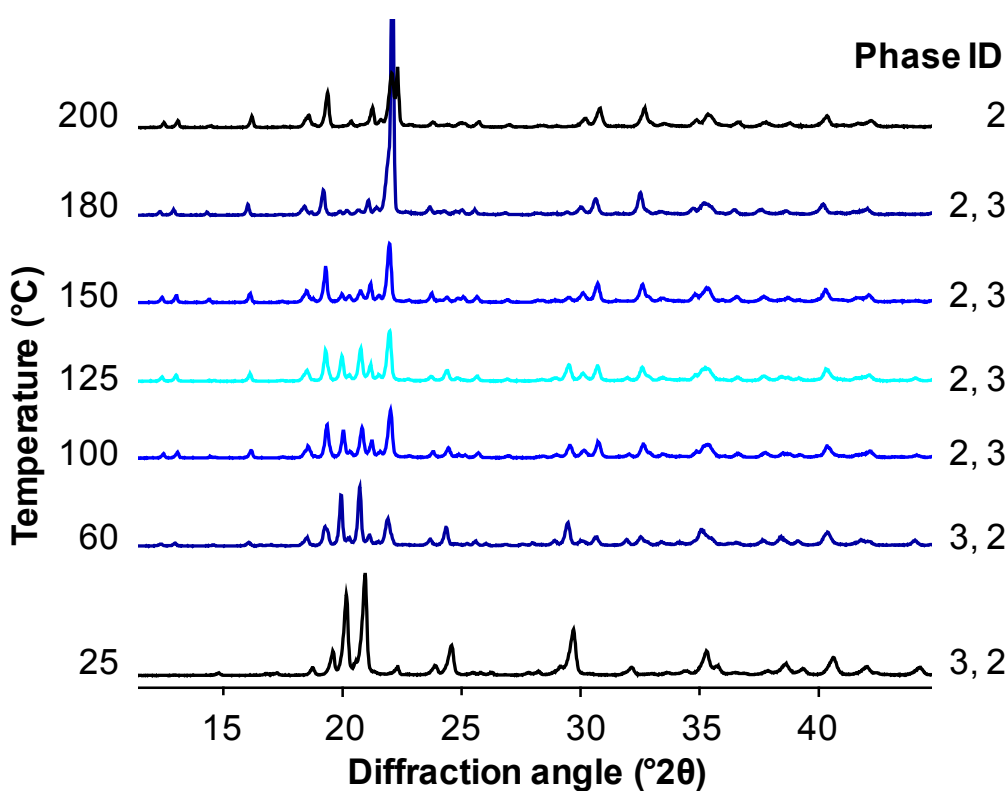


Figure S6. Powder X-ray diffraction of the products from phase investigation reactions of lithium tartrates, from L-tartaric acid in water:ethanol, showing phases in order of abundance.

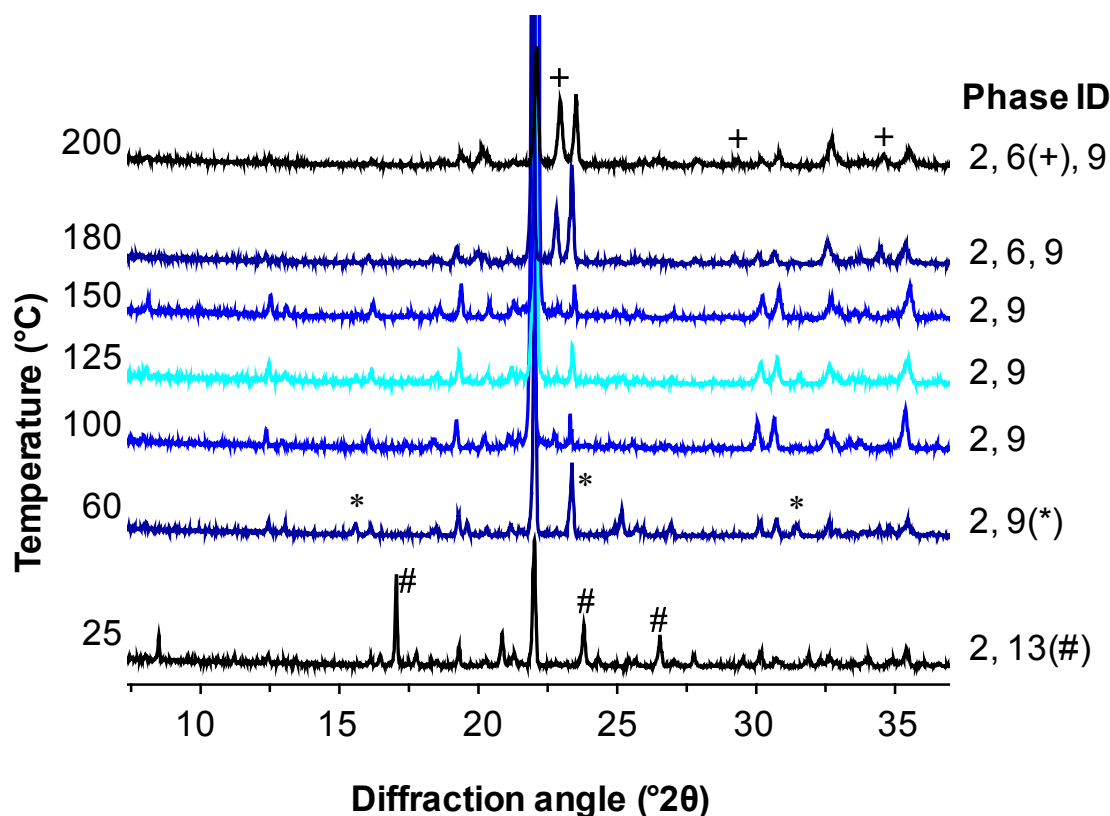


Figure S7. Powder X-ray diffraction of the products from phase investigation reactions of lithium tartrates, from D,L-tartaric acid in ethanol, showing phases in order of abundance.

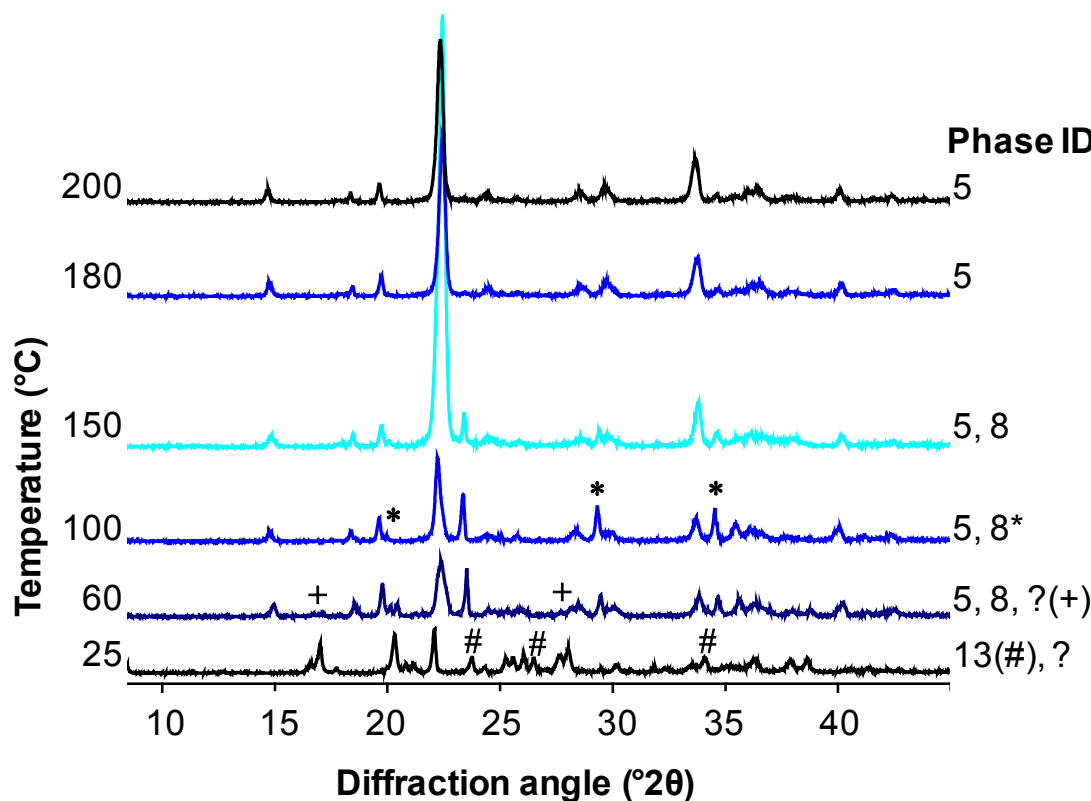


Figure S8. Powder X-ray diffraction of the products from phase investigation reactions of lithium tartrates, from d,l-tartaric acid in water:ethanol, showing phases in order of abundance.

